The 11th Canadian Conference on Earthquake Engineering
Canadian Association for Earthquake Engineering

STRESS-STRAIN CURVE OF CORRODED REINFORCING BARS SUBJECTED TO BUCKLING

Shun SUMINOKURA
Master Program, Dept. of Engineering Mechanics and Energy, University of Tsukuba, Japan
s1420900@u.tsukuba.ac.jp

Teppei MOGAWA
Master Program, Dept. of Engineering Mechanics and Energy, University of Tsukuba, Japan
s1520926@u.tsukuba.ac.jp

Michiaki OYADO, Dr.Eng.
Senior Researcher, Structures Technology Division, Railway Technical Research Institute, Japan
oyado.michiaki.64@rtri.or.jp

Akira YASOJIMA, Ph.D.
Assistant Professor, Dept. of Engineering Mechanics and Energy, University of Tsukuba, Japan
yaojima@kz.tsukuba.ac.jp

Toshiyuki KANAKUBO, Ph.D.
Associate Professor, Dept. of Engineering Mechanics and Energy, University of Tsukuba, Japan
kanakubo@kz.tsukuba.ac.jp

ABSTRACT: This study focuses on the buckling behavior of the corroded reinforcing bars in reinforced concrete. In the previous study, buckling test on scraped reinforcing bars to simulate the corrosion was conducted. However, actual corrosion forms various reductions of the cross-sectional area in longitudinal direction, it is necessary to simulate the corroded reinforcing bars with more variety. Moreover, modeling of stress-strain curve after the maximum stress has not been clearly studied. In this study, buckling tests using non-corroded reinforcing bars, scraped reinforcing bars, and reinforcing bars by electrolytic corrosion were conducted. The buckling strengths and the stress-strain curves of reinforcing bars were investigated by buckling test. In addition, modeling of the stress-strain curve after the maximum stress was proposed based on the experiment results. As a result, the buckling strengths of the scraped reinforcing bars and the reinforcing bars by electrolytic corrosion were influenced by the reduction of the cross-sectional area. The buckling strength of the corroded reinforcing bars was evaluated safely by full plastic strength considering eccentric force. The stress-strain curves after the maximum stress of corroded reinforcing bars could be mostly expressed by a proposed model.

1. Introduction

Recently, the number of RC structures which has passed years from construction has been increasing. There has been recognized deteriorations of aged structure by environmental effect. Corrosion of the reinforcing bar due to salt attack and carbonation has become a typical degradation cause that affects the load resistant behavior of RC structures. Many researches on tensile performance of corroded reinforcing bars have been conducted, while there are few researches on compression performance. In previous studies (Suzuki et al., 2013), the bending loading test of RC beams with corroded reinforcing bars on compression side was conducted. The result pointed out the possibility of brittle destruction by cracking of cover concreate due to corrosion of reinforcing bar and buckling of corroded reinforcing bar. Therefore, focuses on the buckling behavior of the reinforcing bar and buckling test on scraped reinforcing bars to simulate the corrosion of cross-sectional area in longitudinal direction was conducted (Kanakubo et al., 2014). However, actual corrosion forms various reductions of the cross-sectional area in longitudinal direction, it is necessary to simulate the corroded reinforcing bars with more variety. In this study, buckling test using non-corroded reinforcing bars, scraped reinforcing bars, and reinforcing bars by electrolytic corrosion is conducted. The buckling strengths and the stress-strain curves after the maximum stress of reinforcing bars are investigated by buckling test. In addition, modeling of stress-strain curves after the maximum stress is proposed based on the experiment results.

2. Test Outline

2.1. Test Specimen

Deformed bars were used for specimens that were prepared as non-corroded reinforcing bars, scraped reinforcing bars, and reinforcing bars by electrolytic corrosion.

2.1.1. Non-Corroded Reinforcing Bar

Specimen list of non-corroded reinforcing bars is shown in Table 1. Deformed bar of D10 (SD295), D13 (SD295, SD490), and D16 (SD295, SD345) were used. Experimental factors were test length. The test length of the specimen was set as from 8*d* to 20*d* (*d* is the bar diameter) (roughly less than 100 in the effective slenderness ratio).

2.1.2. Scraped Reinforcing Bar

Specimen list of scraped reinforcing bars is shown in Table 2. Tested bars were same as deformed bar of D10 non-corroded reinforcing bar. Test length is 16*d*. In view of the case that corrosion proceeds from the cover concrete surface, specimens have scraped region using a disc sander as shown in Fig. 1.

Table 1 – Specimen list of non-corroded reinforcing bars

Specimen		Test length
D10	SD295	20*d*,18*d*,16*d*,14*d*,12*d*,10*d*,8*d*
D13	SD295	
	SD490	
D16	SD295	
	SD345	

Table 2 – Specimen list of scraped reinforcing bars

Specimen name	Test length *d*:the bar diameter(mm)	Scraped rate(%)		
		U	C	L
U-0,C-15,L-0	16*d*	-	15	-
U-15,C-0,L-15		15	-	15
U-15,C-15,L-15		15	15	15
U-30,C-0,L-0		30	-	-
U-0,C-30,L-0		-	30	-
U-30,C-30,L-0		30	30	-
U-30,C-0,L-30		30	-	30
U-30,C-30,L-30		30	30	30
U-0,C-45,L-0		-	45	-
U-45,C-0,L-45		45	-	45
U-45,C-15,L-45		45	15	45
U-45,C-30,L-45		45	30	45
U-45,C-45,L-45		45	45	45

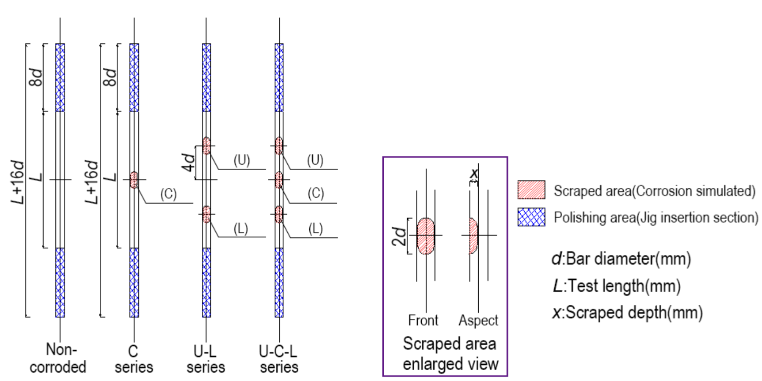

Fig. 1 – Detail of scraped reinforcing bars

Scraped position is varied as central part only (C series), two positions of upper and lower (U-L series), and three positions (U-C-L series). Scraping was carried out by controlling a scraped depth in the minimum diameter direction between lugs of reinforcing bar (Fig. 2). An ellipse having a nominal cross-sectional area is assumed to determine cross-sectional area ratio (scraped rate), which was set to be 15%, 30%,and 45%.

2.1.3. Reinforcing Bars by Electrolytic Corrosion

Six compression side reinforcing bars of RC beams which were subjected to electrolytic corrosion and loading test (Suzuki et al., 2013) were chipped out after loading. Fig. 3 shows the corroded bars after rust removal. Specimen No.1 has the overall corrosion, and specimen No.6 also has overall corrosion with localized corrosion. Cross-sectional area distributions of the specimens were measured using the cross-section measurement method by 3D scanner (Oyado et al., 2006). The measurement results are shown in Fig. 4. Dashed line in the figure shows the average cross-sectional area (67.11mm^2) of the same non-corroded reinforcing bar by 3D scanner. The average cross-sectional area, minimum cross-sectional area and cross-sectional reduction rate (ratio of average cross-sectional area to the non-corroded reinforcing bar) of reinforcing bars by electrolytic corrosion are shown in Table 3. The tensile test results of non-

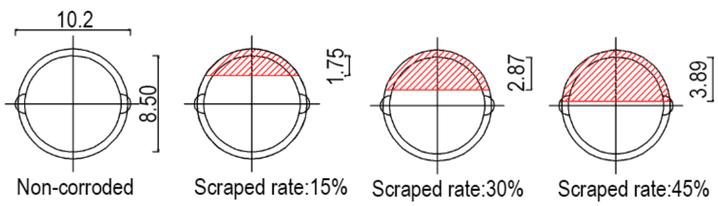

Fig. 2 – Scraped rate and depth

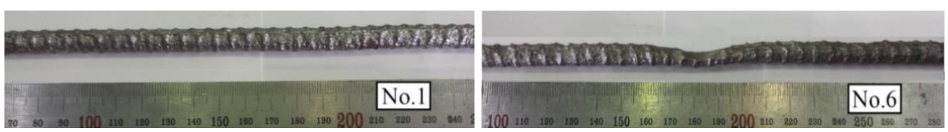

Fig. 3 – Example of appearance of the reinforcing bars by electrolytic corrosion

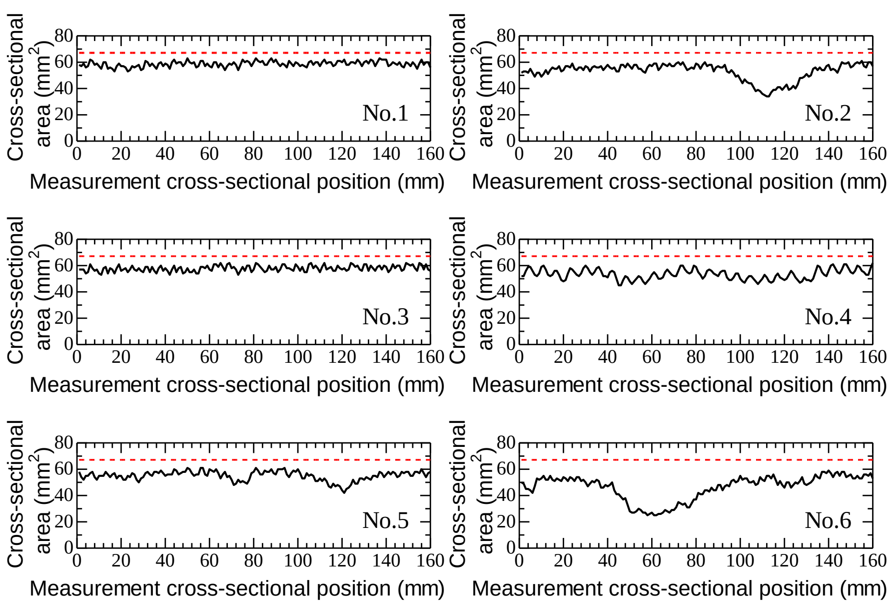

Fig. 4 – Cross-sectional area distribution in the axial direction of the reinforcing bars by electrolytic corrosion

corroded reinforcing bar are shown in Table 4.

2.2. Loading and Measurement Method

Loading and measurement method are shown in Fig. 5. Monotonic compression loading was carried out using a universal testing machine of 500kN capacity. The jigs for fixing specimen were attached to the heads of the testing machine, so the boundary condition was to be fixed-end by inserting the ends of 8*d* of the reinforcing bar in the jigs. The inserted ends of reinforcing bar were polished to produce no gap between the holes of the jigs and the reinforcing bar. Measurement items were compressive force and an axial deformation using LVDTs in three positions between the jigs.

3. Test Result

3.1. Non-Corroded Reinforcing Bar

Specimens after loading and examples of stress-strain curves of non-corroded reinforcing bars are shown Fig. 6 and Fig. 7, respectively. Stress is determined by dividing compressive force by the nominal cross-sectional area. Strain is calculated by dividing axial deformation in test region by test length. The deformation in test region is obtained by subtracting the deformations of the bar in the hole (assumed as elastic) from the measured deformation by LVDT. The specimens showed buckling after reaching yield strength. The buckling occurred around weak axis, which corresponds to the direction between longitudinal ribs in the section. As the test length becomes smaller, yield plateau is clearly observed and the stress-strain curve after the maximum stress shows more gradual declivity.

Table 3 – Cross-sectional area of the reinforcing bars by electrolytic corrosion

Specimen name	Test length *d*:the bar diameter(mm)	Minimum cross-sectional area		Average cross-sectional area	
		(mm^2)	Reduction rate(%)	(mm^2)	Reduction rate(%)
No.1	16*d*	52.79	21.34	58.66	12.60
No.2		34.25	48.96	52.95	21.10
No.3		53.32	20.54	57.86	13.79
No.4		44.59	33.55	53.32	20.55
No.5		42.38	36.84	55.06	17.96
No.6		24.99	62.76	46.29	31.02

Table 4 – Tensile test results

Specimen		Ultimate tensile strength (MPa)	Yield strength (MPa)	Elastic modulus (GPa)	Yield strain (%)
D10	SD295	468 (538)	346 (400)	192 (188)	0.178 0.215
D13	SD295	484	344	192	0.178
	SD490	707	565	196	0.295
D16	SD295	482	334	197	0.174
	SD345	516	358	198	0.190

( ): test result of reinforcing bar used for electrolytic corrosion

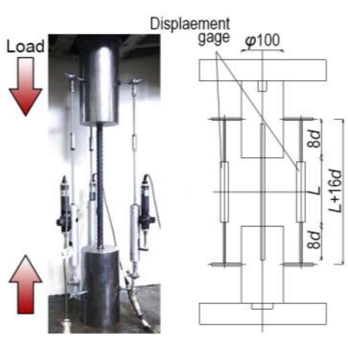

Fig. 5 – Loading and measurement method

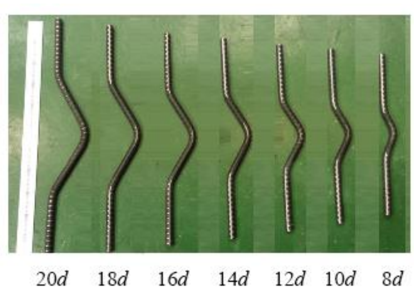

Fig. 6 – Non-corroded reinforcing bar after loading

3.2. Scraped Reinforcing Bar

Examples of scraped reinforcing bars after loading are shown in Fig. 8. The buckling occurred showing largest lateral deformation at the scraped position with the minimum cross-sectional area. In case of having two or three positions with the same minimum cross-sectional area including the center, the buckling occurred showing largest lateral deformation at the center position. Examples of stress-strain curves of scraped reinforcing bar are shown Fig. 9. Examples of normalized stress-strain curves by the maximum stress of each specimen are shown in Fig. 10. As the reduction ratio of the cross-sectional area increases, the maximum stress decreases, and the stress-strain curve after the maximum stress shows more gradual declivity. The differences of stress-strain curves after the maximum stress are observed depending on the belly position of buckling mode. The reason of that is considered that the belly position affects the bending stiffness of reinforcing bar. In case of that the belly is in the center of test region, the stress-strain curve after the maximum stress shows steep declivity. The relation between cross-section reduction rate and the buckling load ratio (ratio of buckling load to non-corroded reinforcing bar) of scraped reinforcing bar is shown in Fig. 11. Buckling strength is evaluated by the yield strength for two cases, i.e. (1) in consideration of cross-section reduction in the scraped position, and (2) in consideration of the full plastic moment (Fig. 12) by the eccentric load of scraped section. These evaluations are indicated by lines in Fig. 11. The case (2) is considered taking into account to the eccentricity of the acting force. The strength is calculated by section analysis under the assumption that the stress distribution of

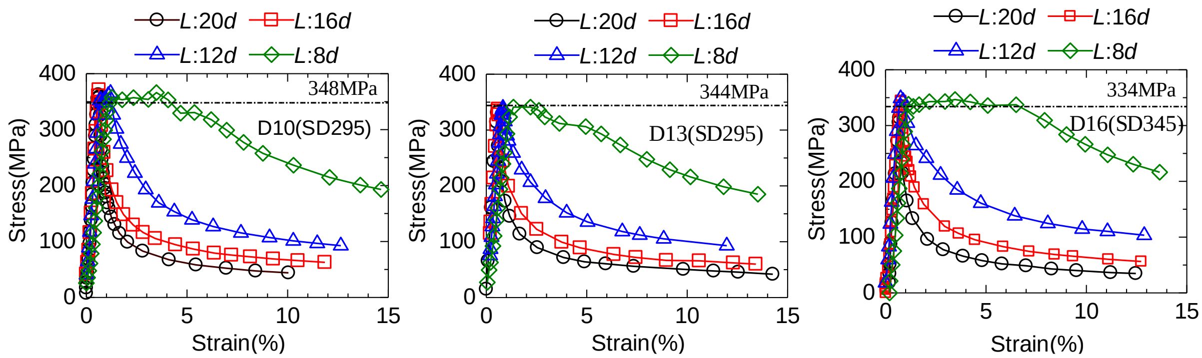

Fig. 7 – Example of stress-strain curve of non-corroded reinforcing bar

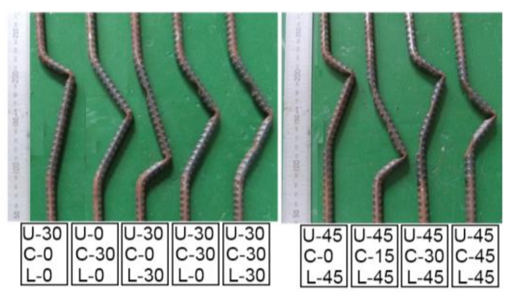

Fig. 8 – Scraped reinforcing bar after loading

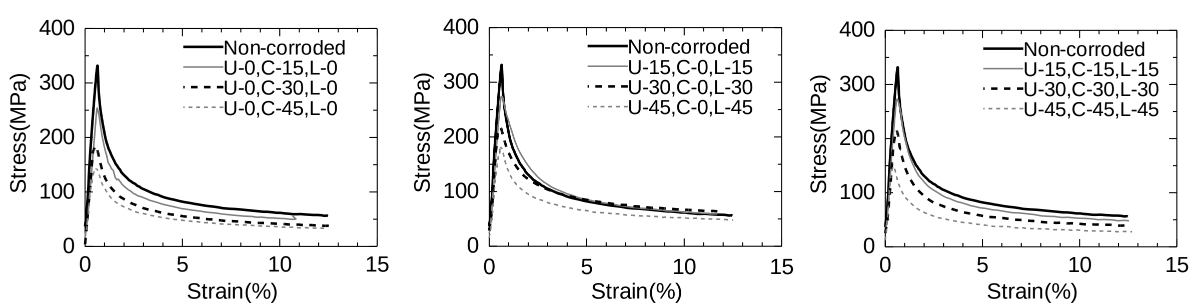

Fig. 9 – Example of stress-strain curve of scraped reinforcing bar

compression and tension side in the scraped section exhibits full plastic state. The test results can be evaluated in the safe side in the yield strength (2).

3.3. Reinforcing Bars by Electrolytic Corrosion

The stress-strain curves of reinforcing bars by electrolytic corrosion are shown in Fig. 13. Maximum stress decreased as well as the increase of reduction ratio of cross-sectional area. The relationship of cross-section reduction rate and buckling load ratio is shown in Fig. 14. It is considered that the buckling load can be evaluated in the safe side by the yield strength (2) using a cross-section reduction rate by the minimum cross-sectional area measured by the 3D scanner. It is assumed that the corroded reinforcing bars in the actual structure have various form of corrosion. However, the yield strength (2) is considered to represent the lower limit of the buckling load in consideration of the uneven distribution of corrosion.

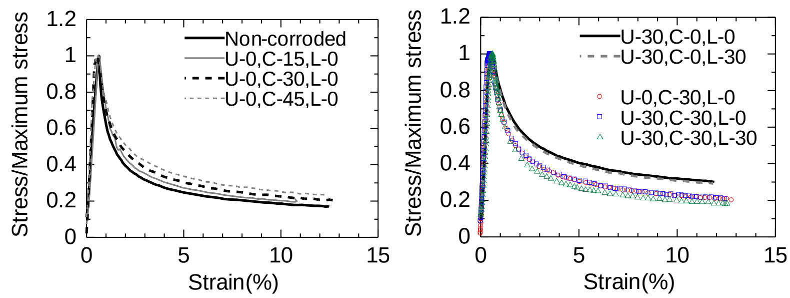

Fig. 10 – Example of normalized stress-strain curve of scraped reinforcing bar

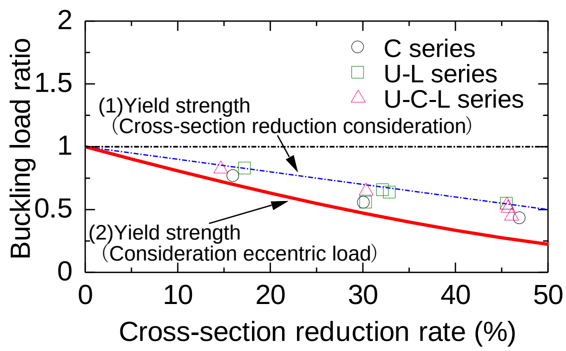

Fig. 11 – Relation between cross-section reduction rate and buckling load ratio of scraped reinforcing bar

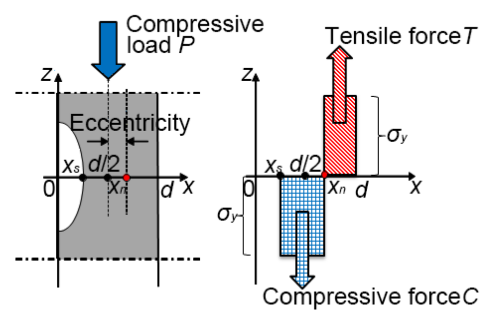

Fig. 12 – Evaluation of the yield strength by the eccentric load of scraped section

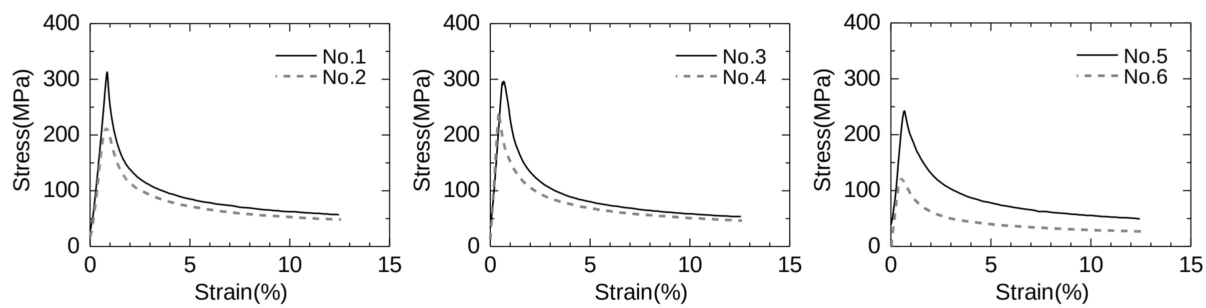

Fig. 13 – Stress-strain curve of reinforcing bar by electrolytic corrosion

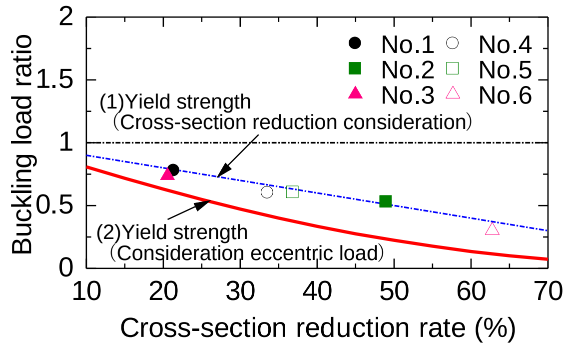

Fig. 14 – Cross-section reduction rate and buckling load ratio by electrolytic corrosion

4. Model of Stress-Strain Curve after Maximum Stress

4.1. Method of Modeling

4.1.1. Non-Corroded Reinforcing Bar

The stress-strain curve after the maximum stress is formulated by Equation (1). β is a coefficient representing the difference in the stress-strain curve after the maximum stress. It is evaluated by the function of the test length from the experimental results. In case that the yield plateau is not observed, the buckling strength (σ_b) and buckling strain (ε_b) are given as the maximum stress and strain at the maximum stress, respectively. In the case of specimens with yield plateau, the strain at yield point (σ_y) on the stress-strain curve is defined as ε_y' , σ_b is replaced by the average value of the stress between ε_y -ε_y' as shown in Fig. 15. The strain at the intersection with σ_b is substituted for ε_b. The value of β for each specimen is determined by the least-square method by the stress-strain curve after the maximum stress. The relationship between the value of β and the test length by bar diameter is shown in Fig. 16. As the test length reduces, the value of β decreases, that expresses the tend that the stress-strain curve after the buckling stress shows more gradual declivity. The relation is formulated in Equation (2) by the least-square method using the results of all specimens.

$$\sigma = \sigma_b(\varepsilon_b / \varepsilon) \tag{1}$$

$$\beta = 0.049(L / d) \tag{2}$$

Where, σ_b: buckling strength, ε_b: buckling strain, L: test length, d: bar diameter.

The relationship between buckling strain ε_b and the test length divided by the bar diameter is shown in Fig. 17. The buckling strain ε_b is standardized by yield strain $\varepsilon_{y,t}$ obtained by tensile test. The buckling strain increases with the reduction of test length. The relation is formulated by Equation (3) by the least-square method using the results of all specimens.

$$\varepsilon_b = \varepsilon_{y,t} e^{21.7/(L/d)} \tag{3}$$

Where, $\varepsilon_{y,t}$: yield strain in tensile test.

4.1.2. Scraped Reinforcing Bar and Reinforcing Bars by Electrolytic Corrosion

From the test results, the stress-strain curve after the maximum stress shows more gradual declivity by increasing the cross-section reduction rate. This phenomenon is introduced into Equation (1) in consideration of the reduction of the minimum cross-sectional area. As a result, Equation (4) is derived.

$$\sigma = \sigma_b(\varepsilon_b / \varepsilon)^{\beta\sqrt{1-\alpha/100}} \tag{4}$$

Where, α: reduction of the minimum cross-sectional area.

4.2. Comparison of Test Results and Model

Comparisons of the test results and the proposed model are shown in from Fig. 18 to Fig. 20. Stress is normalized by σ_b. The proposed model is appropriate for simulating the stress-strain curves after the maximum stress of non-corroded reinforcing bar, scraped reinforcing bar and reinforcing bars by electrolytic corrosion.

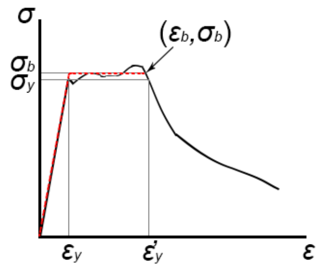

Fig. 15 – Definition of σ_b and ε_b

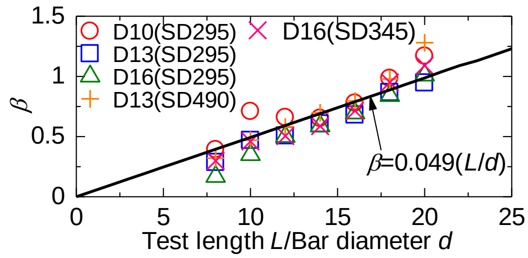

Fig. 16 – Relationship between β and test length by bar diameter

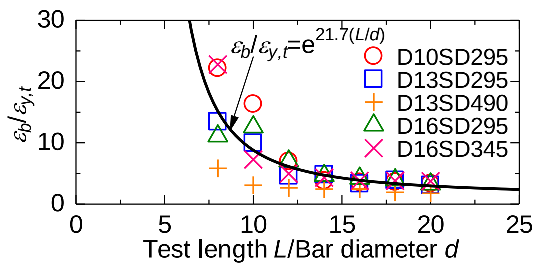

Fig. 17 – Evaluation of buckling strain

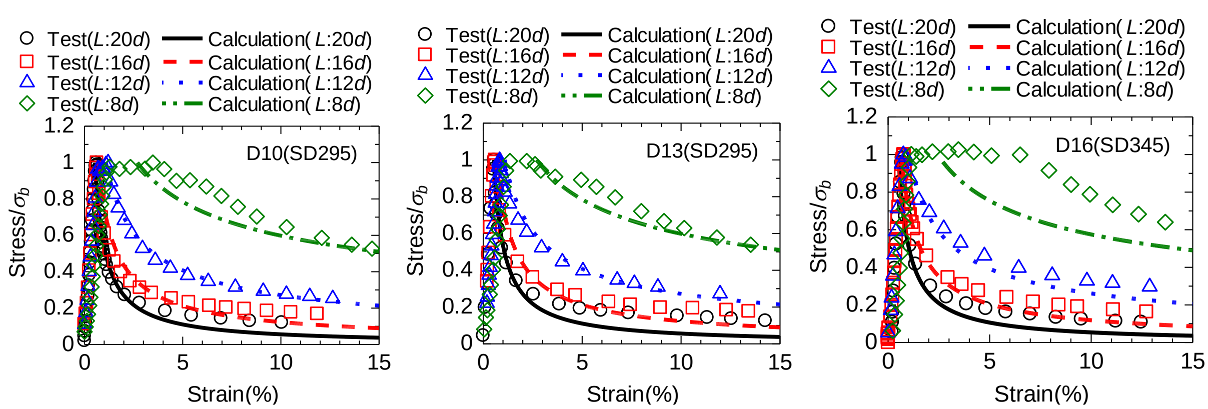

Fig. 18 – Comparison of test results and proposed model in non-corroded reinforcing bar

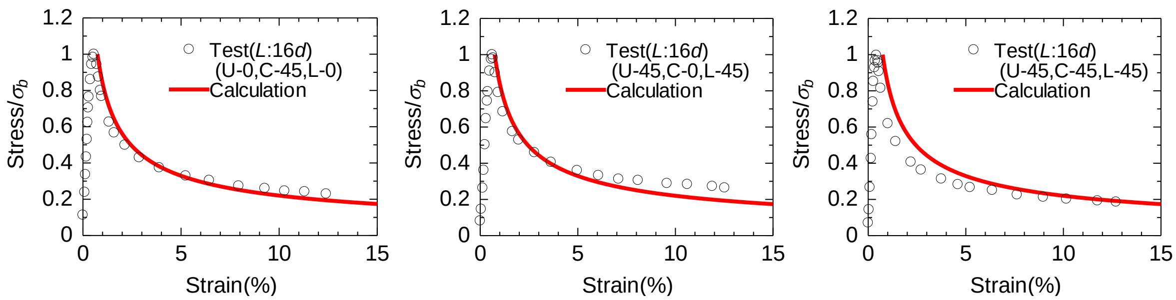

Fig. 19 – Comparison of test results and proposed model in scraped bar

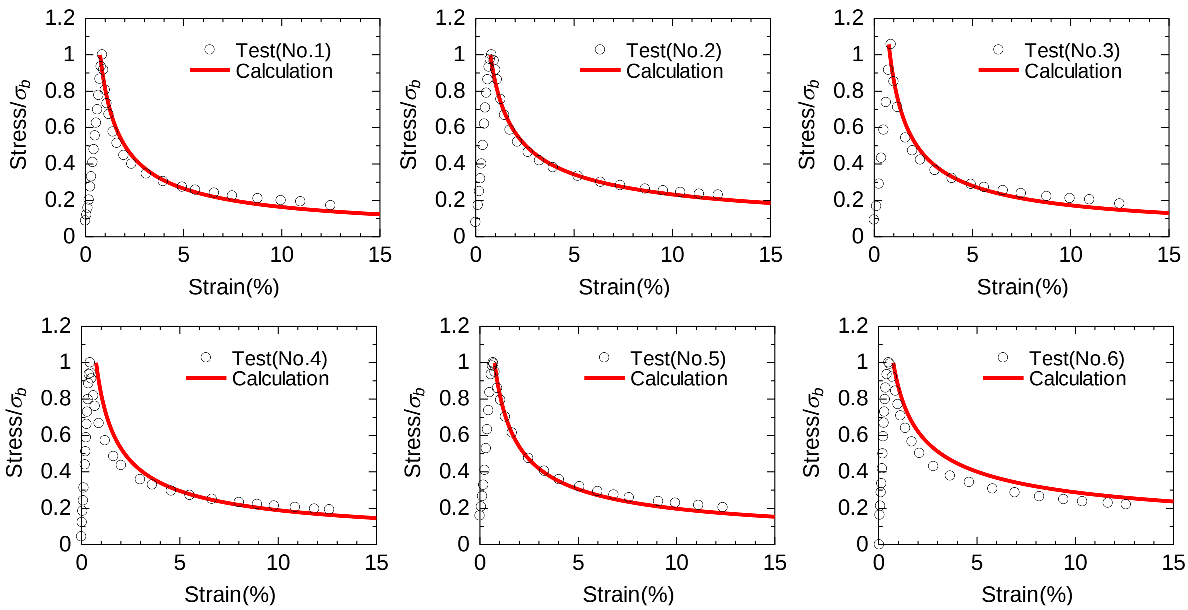

Fig. 20 – Comparison of test results and proposed model in reinforcing bar by electrolytic corrosion

5. Conclusion

The buckling occurred showing largest lateral deformation at the scraped position with the minimum cross-sectional area. The maximum stress decreases with the increase of the reduction ratio of the cross-sectional area, and the stress-strain curve after the maximum stress shows more gradual declivity. In consideration of the full plastic moment by the eccentric load of scraped section, buckling strength of scraped bars can be evaluated in the safe side. Also in reinforcing bars by electrolytic corrosion, buckling load can be evaluated using the reduction of the minimum cross-sectional area measured by the 3D scanner. Modeling of stress-strain curve after the maximum stress was proposed based on the experiment results. The comparison of simulated result and observed result showed that the proposed model is appropriate for modelling the stress-strain curves of non-corroded reinforcing bar, scraped reinforcing bar and reinforcing bars by electrolytic corrosion.

6. Acknowledgements

This study was supported by the JSPS KAKENHI Grant Number 24560593.

7. References

KANAKUBO, Toshiyuki, YASOJIMA, Akira, OYADO, Michiaki, TAKEDA, Atsushi, SUZUKI, kenji, “ Buckling Behavior of the Scraped Reinforcement Simulating Corrosion“, *Proceedings of the 69th Annual Conference of the Japan Society of Civil Engineers*, September 2014, pp. 905-906. (in Japanese)

OYADO, Michiaki, KANAKUBO, Toshiyuki, YAMAMOTO, Nobuyuki, SATO, Tsutomu, ”Influence of Corrosion of Reinforcing Bars on Bending Performance of Reinforced Concrete Members”, *JSCE Joumal of Materials, Concrete Structures and Pavements, Division E,* Vol.62, No.3, August 2006, pp. 542-554. (in Japanese)

SUZUKI, Kenzi, KANAKUBO, Toshiyuki, YASOJIMA, Akira, OYADO, Michiaki, “Bending Behavior of RC Beams with Corroded Compression Reinforcing Bar”, *Japan Concreate Institute Symposium on Unified System to Evaluate Structure and Durability Performance in Corroded RC Structure,* November 2013, pp. 259-264. (in Japanese)